

Initial state fluctuations in p+A and A+A collisions and their influence on geometry measures



Jan Kochanowski
University

Grzegorz Stefanek¹, Wojciech Broniowski^{1,2}, Maciej Rybczyński¹

¹Jan Kochanowski University, Kielce, Poland

²Institute of Nuclear Physics, Kraków, Poland



Introduction

Fluctuations in physics observables and flow effects in heavy-ion collisions have been topics of particular interest in recent years as they may provide important signals regarding the formation of quark-gluon plasma, the existence of critical point and the evolution of the system. The fluctuations and correlations measured in the final stage have their sources at least partly in the initial-state geometry and initial "geometric" fluctuations.

Variants of the Glauber model, in particular the wounded-nucleon model and its extensions, have become a basic tool in modeling the early stage of relativistic heavy-ion collisions. The Glauber model approach provides initial conditions for the subsequent hydrodynamic evolution. That way the features of nuclei structure, such as distributions of nucleons in nuclei, the nucleus deformation, the nucleon-nucleon correlations, as well as NN cross section show up indirectly in the measured observables.

GLISSANDO

GLISSANDO [1] is a Glauber Monte-Carlo generator for initial stages of relativistic heavy-ion collisions. Several models were implemented in GLISSANDO: the wounded-nucleon model, the binary collisions model, the mixed model, and the model with hot-spots. The nucleon-nucleon collision at the impact parameter b can be represented in GLISSANDO by hard-sphere, gaussian or gamma approximations with different fluctuations of cross section measured by scaled variance ω . The program generates, among others, the variable-axes (participant) two- and three-dimensional profiles of the density of sources in the transverse plane and their Fourier components. These profiles are used for the further analyses of physics phenomena.

The new features implemented in GLISSANDO 2 [2] include:

- parametrization of shape of all typical nuclei including light nuclei ^3He - ^{16}O (a harmonic oscillator shell model density) especially useful in applications for the NA61 experiment [3]
- inclusion of the deformation of the colliding nuclei according the deformed Woods-Saxon density. The deformation effects are relevant for the collisions of deformed Au and U nuclei recently used at RHIC
- possibility of using correlated distributions of nucleons in nuclei
- possibility of overlaying distributions of the produced particles which depend on the space-time rapidity
- inclusion of the negative binomial overlaid distribution in addition to the Poissonian and Gamma distributions (different NN wounding profiles)
- inclusion of core-corona effect

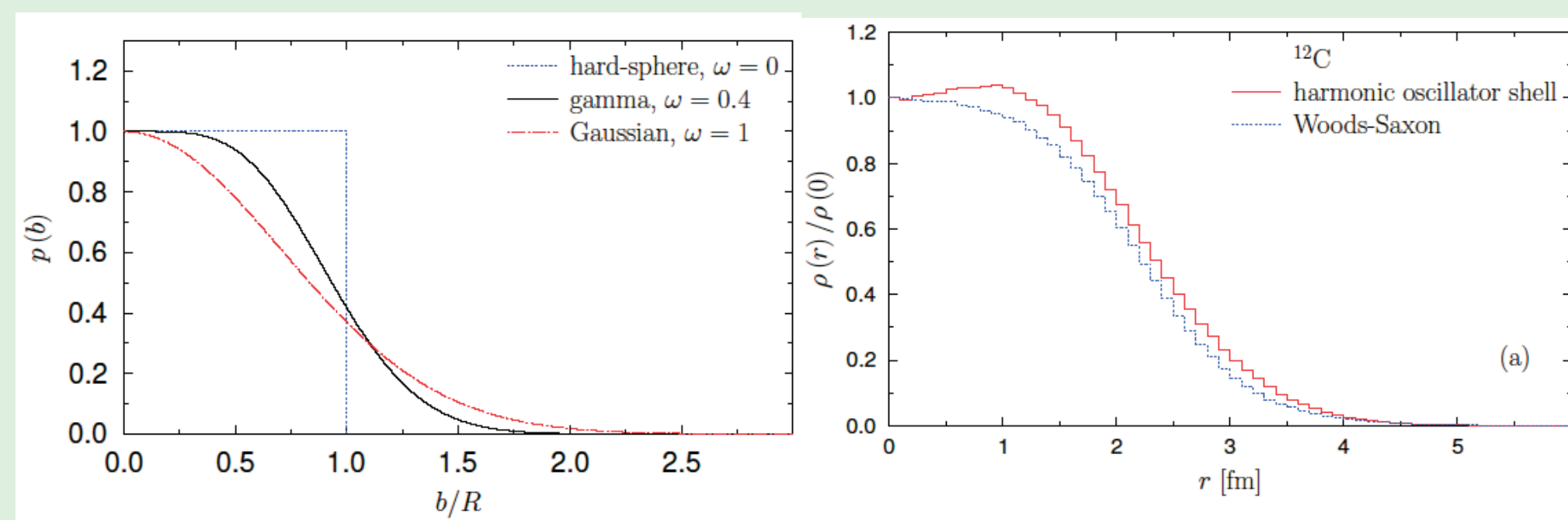


Fig.1 Left: Nucleon-nucleon wounding profile function $p(b)$ for hard-sphere, Gaussian and gamma profiles. Gamma approximation with parameter $\omega = 0.4$ corresponds to the shape of profile function which reproduces well the TOTEM [4] data on elastic differential cross section measure in proton-proton interactions at $\sqrt{s_{NN}} = 7000$ GeV. **Right:** The comparison between nuclear density productions given by harmonic oscillator shell model and Woods-Saxon parametrization for ^{12}C nucleus.

Event plane correlations

Within the Glauber approach, during the first stage of the collision individual interactions between the nucleons deposit transverse entropy (or energy). These elementary processes stemming from wounded nucleons or binary collisions are termed *sources*. A weight called relative deposited strength (RDS) is assigned to each source. The distribution takes the form $f(\text{RDS}) = (1 - \gamma) N_W/2 f_W + N_{bin} f_{bin}$ where γ controls the relative weight of wounded to binary sources.

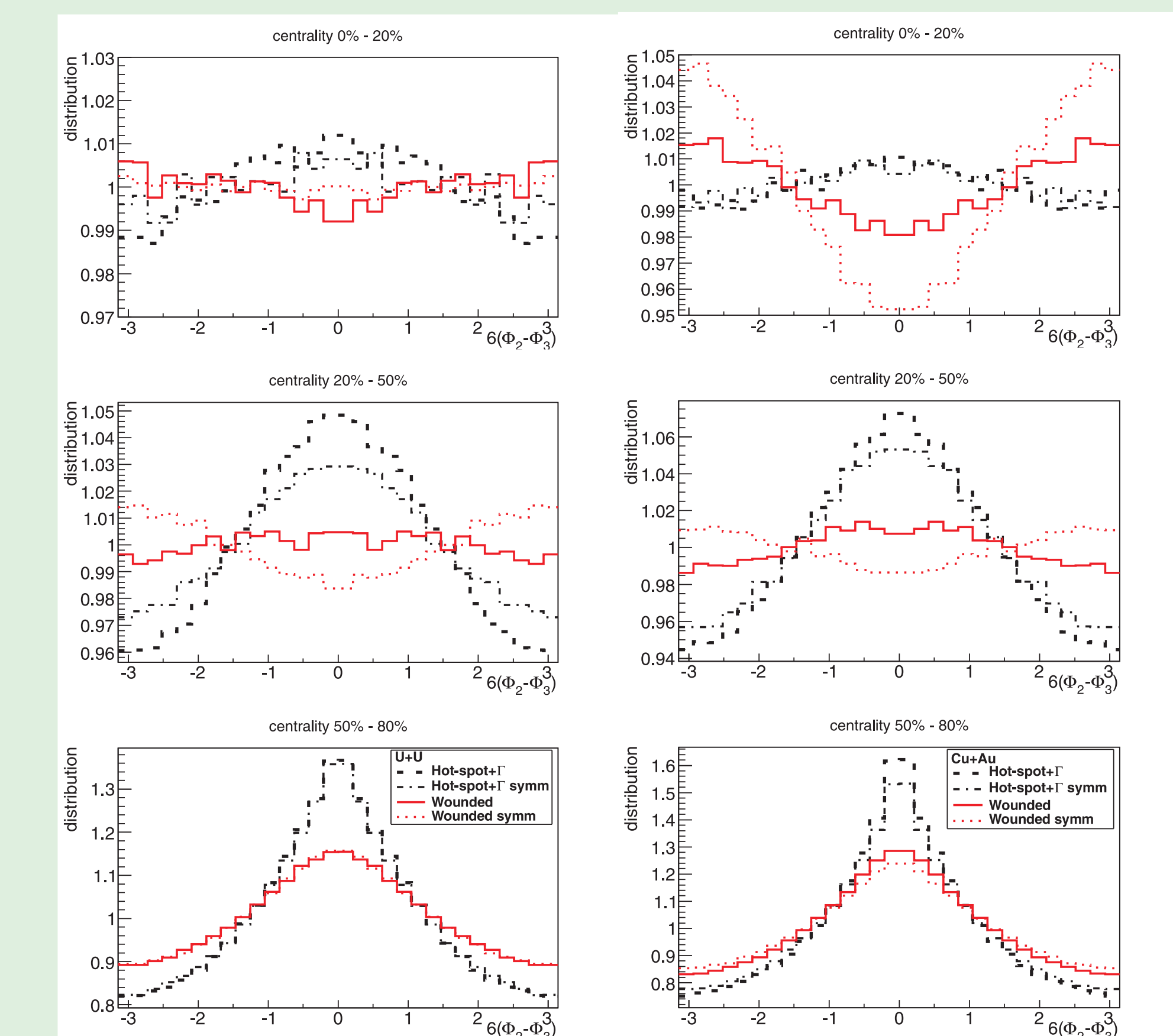


Fig.2 Wounded-nucleon (solid for deformed, dotted for spherical distributions) and hot-spot + (dashed for deformed, dash-dotted for spherical distributions) model prediction for the distribution of $6(\Phi_2 - \Phi_3)$ in U+U (left) and Cu+Au (right) collisions.

For simulated $^{63}\text{Cu} + ^{197}\text{Au}$ and $^{238}\text{U} + ^{238}\text{U}$ the correlation between directions Φ_n of principal axes was studied [5]. The most interesting is the correlation of the lowest-rank even and odd axes, i.e. Φ_2 and Φ_3 (Fig.2). For the wounded-nucleon model these distributions exhibit a maximum at $\Phi_2 - \Phi_3 = 0$ in central collisions. This can be understood as follows: The angle Φ_2 fluctuates around the direction perpendicular to the reaction plane. The triangularity angle Φ_3 naively should be completely random. However, since in the colliding systems there are more nucleons distributed in the direction parallel to the reaction plane than perpendicular, there is a higher probability that one of the corners of the triangle points in the direction parallel to the reaction plane. The centrality dependence of $\langle \cos[k(\Phi_n - \Phi_m)] \rangle$ for different choices of n and m is shown in Fig.3. The shape of distributions differs for different models. The difference is most visible for the correlation of Φ_2 and Φ_4 .

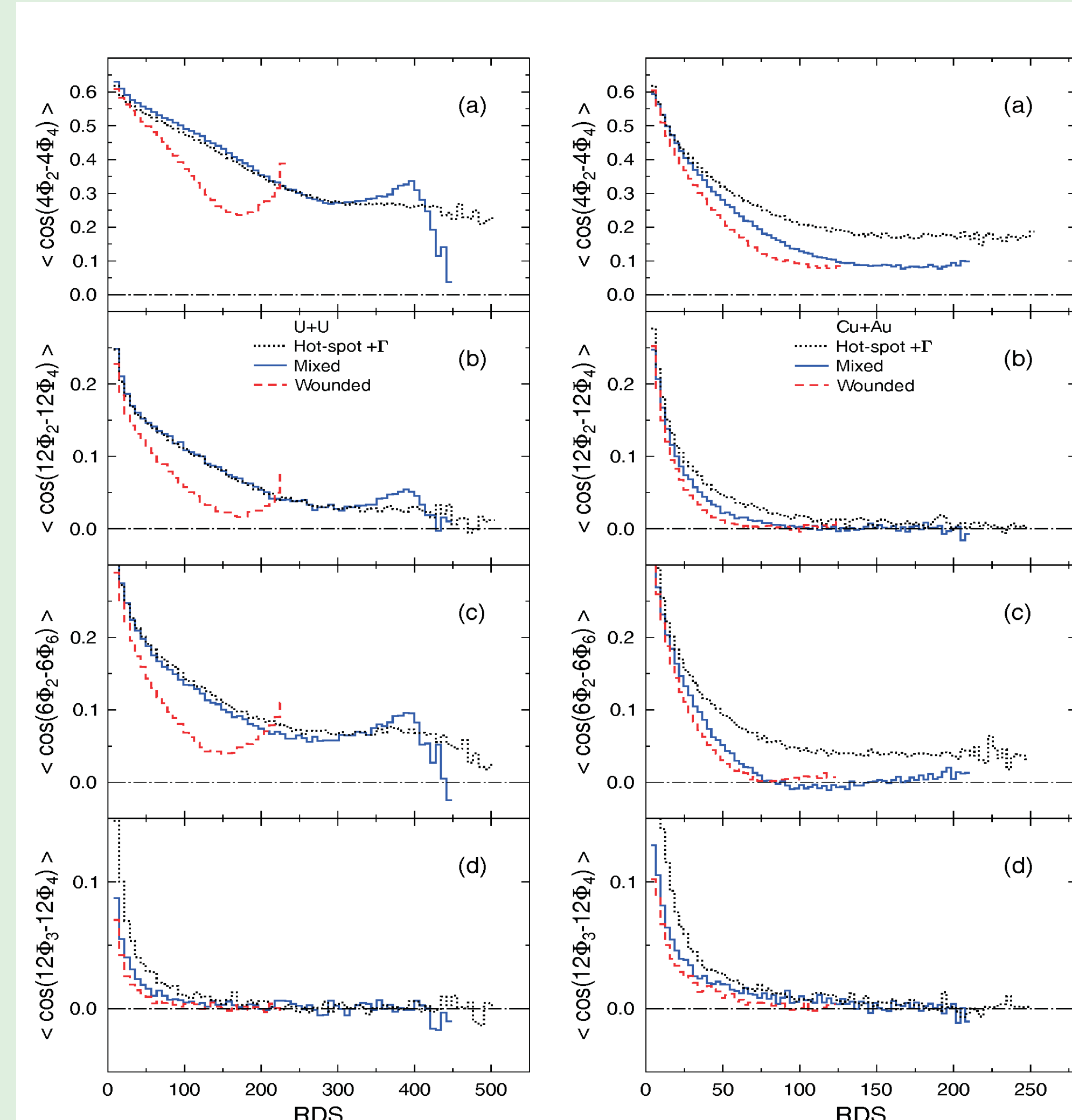


Fig.3 Event-plane correlations measures $\langle \cos[k(\Phi_n - \Phi_m)] \rangle$ for U+U (left) and Cu+Au (right) collisions. The comparison of the predictions of the mixed model (solid line), the wounded-nucleon model (dashed line), and the hot-spot + Γ model (dotted line).

Fluctuations of the number of target participants

The model was used to estimate the mean number of target participants $\langle N_p^{\text{targ}} \rangle$ for production reactions of protons with different targets ^{12}C , ^{14}N , ^{63}Cu , ^{208}Pb at three different energies $\sqrt{s_{NN}} = 5.12, 16.83, 7000$ GeV [6]. Since the production processes are considered, thus the values of $\sigma_{NN}^{\text{inel}}$ are used. As shown in Fig.4 the mean number of target participants may be described by power-law formula $\langle N_p^{\text{targ}} \rangle = N_0 A^\alpha$ with parameter α slightly increasing with energy.

The fluctuations of the number of target participants (N_p^{targ}) were measured by the scaled variance of distributions of N_p^{targ} defined as $\omega_p^{\text{targ}} = \text{Var}(N_p^{\text{targ}}) / \langle N_p^{\text{targ}} \rangle$. Fig. 4 (right) shows that for SPS energies $\sqrt{s_{NN}} = 5.12, 16.83$ GeV, the value of ω_p^{targ} is of the order of unity for p+ ^{63}Cu interactions, which corresponds to the number of target participants given by the Poisson distribution. For p+ ^{12}C and p+ ^{14}N reactions, ω_p^{targ} has values significantly lower than one, whereas for p+ ^{208}Pb - slightly higher. For LHC energy the value of ω_p^{targ} starts around unity for p+ ^{12}C and grows up to $\omega_p^{\text{targ}} \approx 4$ for p+ ^{208}Pb interactions.

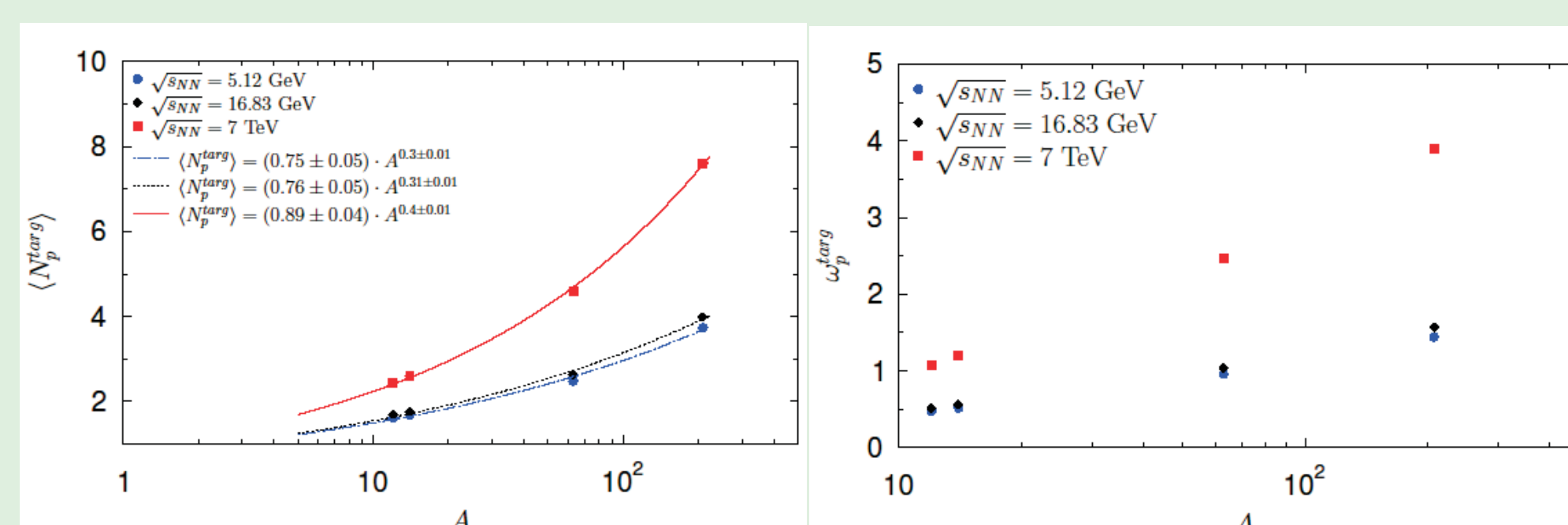


Fig.4 Left: The mean number of target participants $\langle N_p^{\text{targ}} \rangle$ as a function of target atomic mass A . **Right:** Scaled variance of the distribution of target participants number, ω_p^{targ} as a function of target atomic mass A . The results of the GLISSANDO simulation for production reactions of protons with ^{12}C , ^{14}N , ^{63}Cu , ^{208}Pb ions at $\sqrt{s_{NN}} = 5.12, 16.83$ and 7000 GeV.

The simulations were also done for A+A collisions of different nuclei. Fig.5(left) shows the probability distributions, $P(N_p^{\text{targ}})$ of the number of target participants scaled by the projectile mass number A^{proj} . Shapes of considered distributions are similar for all systems except for $^7\text{Be} + ^9\text{Be}$ collisions at SPS energies which slightly differ from distributions for other systems. Fig.5(right) shows a ratio of the mean number of target participants $\langle N_p^{\text{targ}} \rangle$ to projectile participants N_p^{proj} as a function of $N_p^{\text{proj}}/A^{\text{proj}}$. The plotted ratio is slightly above unity for peripheral collisions while it starts to be below one for central collisions.

Following particular interest of the NA61/SHINE Collaboration with fluctuation/correlation studies in search for the critical point, the scaled variance ω_p^{targ} as a function of $N_p^{\text{proj}}/A^{\text{proj}}$ is shown in Fig.6(left). There is non-monotonic behavior of ω_p^{targ} with the maximum located in peripheral collisions for all simulated systems at all considered energies. Fig.6(right) presents the influence of the shape of the wounding profile for the fluctuations of the number of target participants in $^{40}\text{Ar} + ^{45}\text{Sc}$ collisions. The highest fluctuations are observed for the hard-sphere wounding profile at all energies.

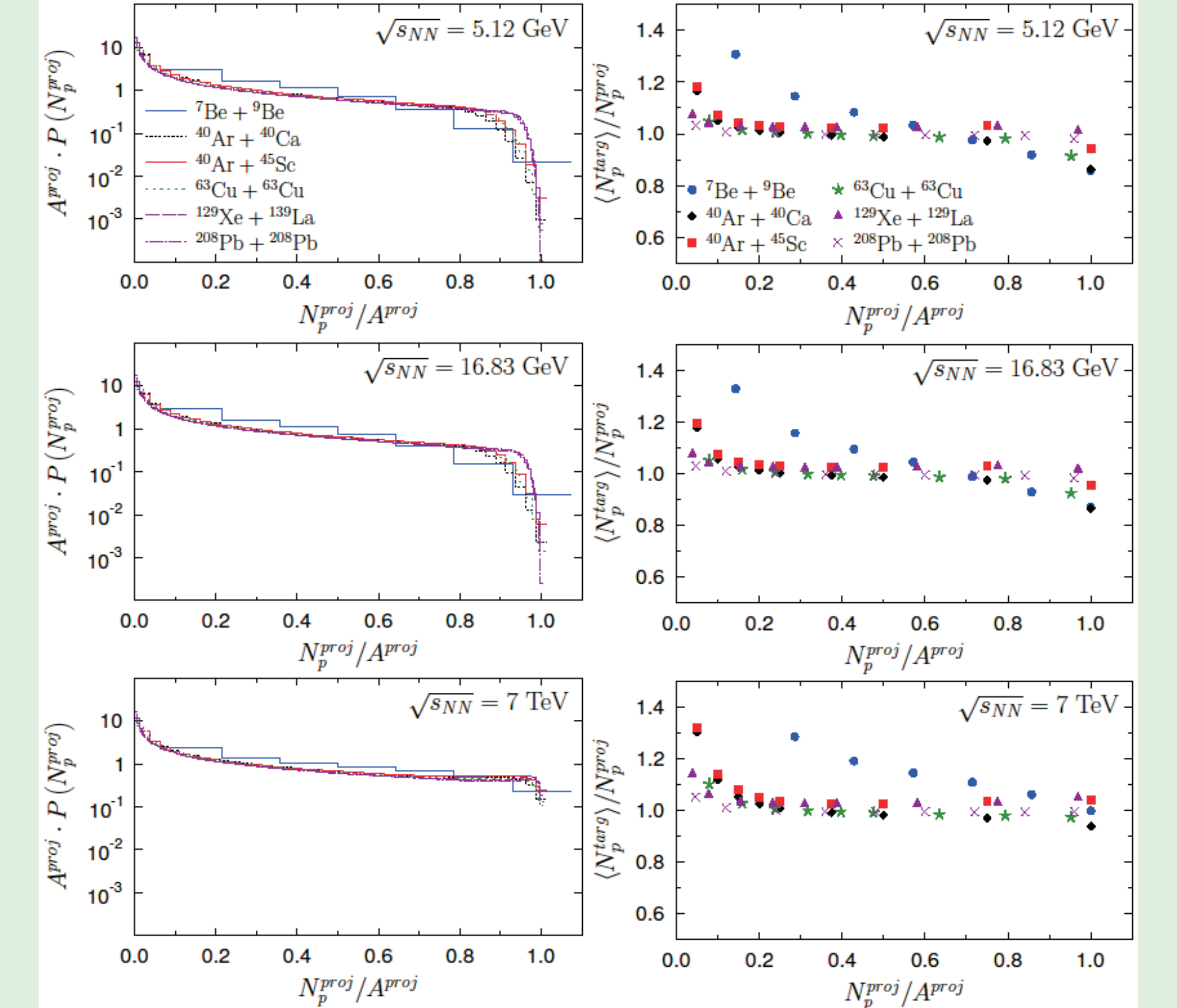


Fig.5 Left: Probability distribution of the number of projectile participants $P(N_p^{\text{proj}})$, scaled by the projectile nucleus mass number, A^{proj} . **Right:** Ratio of the mean number of target participants $\langle N_p^{\text{targ}} \rangle$ to projectile participants N_p^{proj} as a function of $N_p^{\text{proj}}/A^{\text{proj}}$. The results of GLISSANDO simulations for production reactions of various ions at $\sqrt{s_{NN}} = 5.12, 16.83$ and 7000 GeV (the wounded-nucleon model with wounding profile given by the hard-sphere approximation).

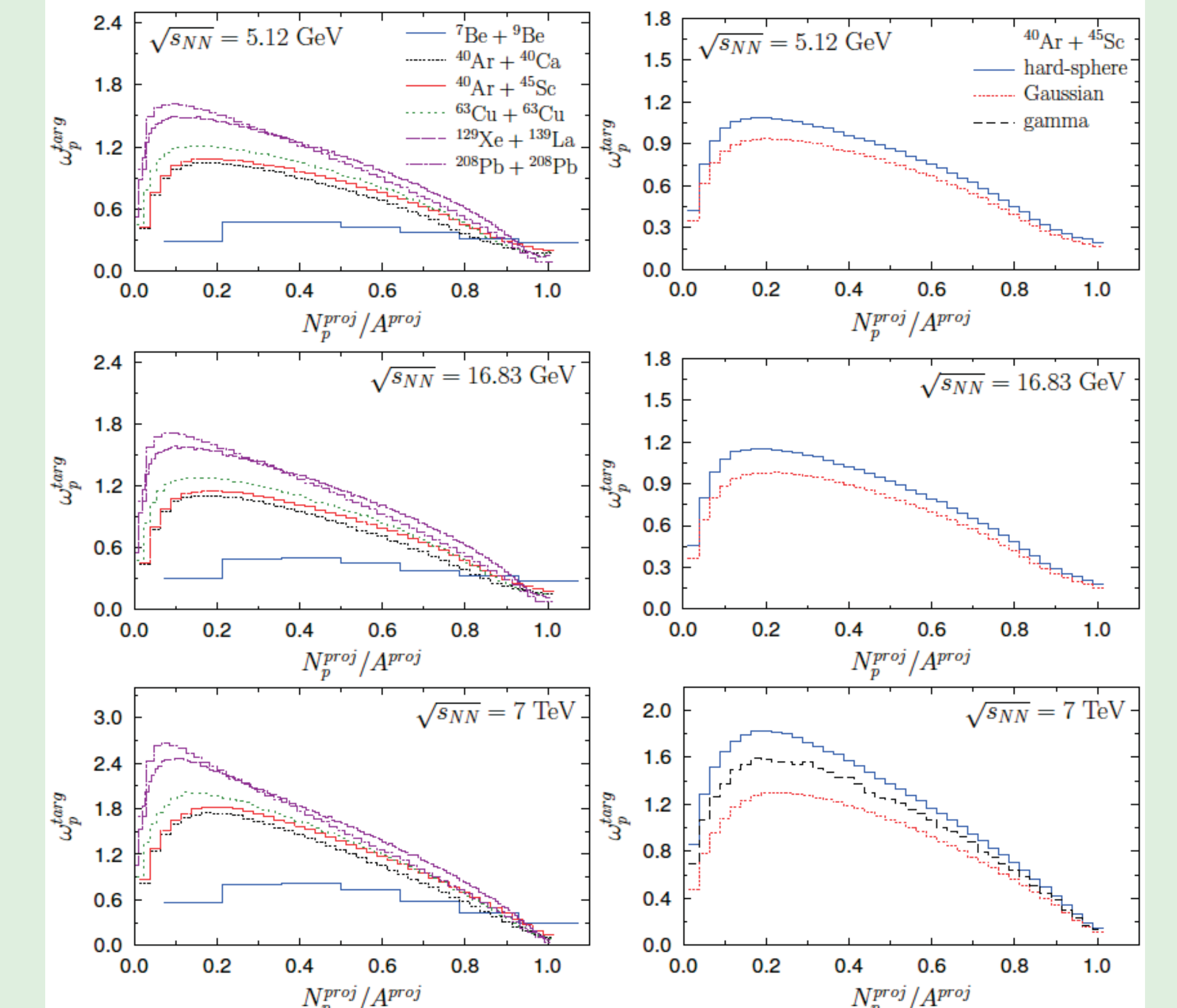


Fig.6 Scaled variance of the number of target participants as a function of $N_p^{\text{proj}}/A^{\text{proj}}$. The results of GLISSANDO simulation for production reactions of various ions at $\sqrt{s_{NN}} = 5.12, 16.83$ and 7000 GeV (the wounded-nucleon model). **Left:** Simulations with the wounding profile given by the hard-sphere approximation. **Right:** Simulations for $^{40}\text{Ar} + ^{45}\text{Sc}$ production reactions with the wounding profile given by the hard-sphere, Gaussian, and gamma approximation.

Cross sections

GLISSANDO simulations were also used to predict proton-nucleus production cross section, $\sigma_{p+A}^{\text{prod}}$. Fig.7 (left) presents proton-nucleus production cross section $\sigma_{p+A}^{\text{prod}}$ as a function of target mass A . The target mass dependence may be described by power-law formula as in the case of average number of target participants, see Fig.4(left). Glauber Monte-Carlo prediction for inelastic $^7\text{Be} + ^9\text{Be}$ cross sections, Fig.7(right), $\sigma_{\text{Be+Be}}^{\text{inel}}$ is consistent with values measured by the NA61/SHINE [7]. As a low energy reference point, the inelastic $^7\text{Be} + ^9\text{Be}$ cross section measured at $\sqrt{s_{NN}} = 2.24$ was used [8].

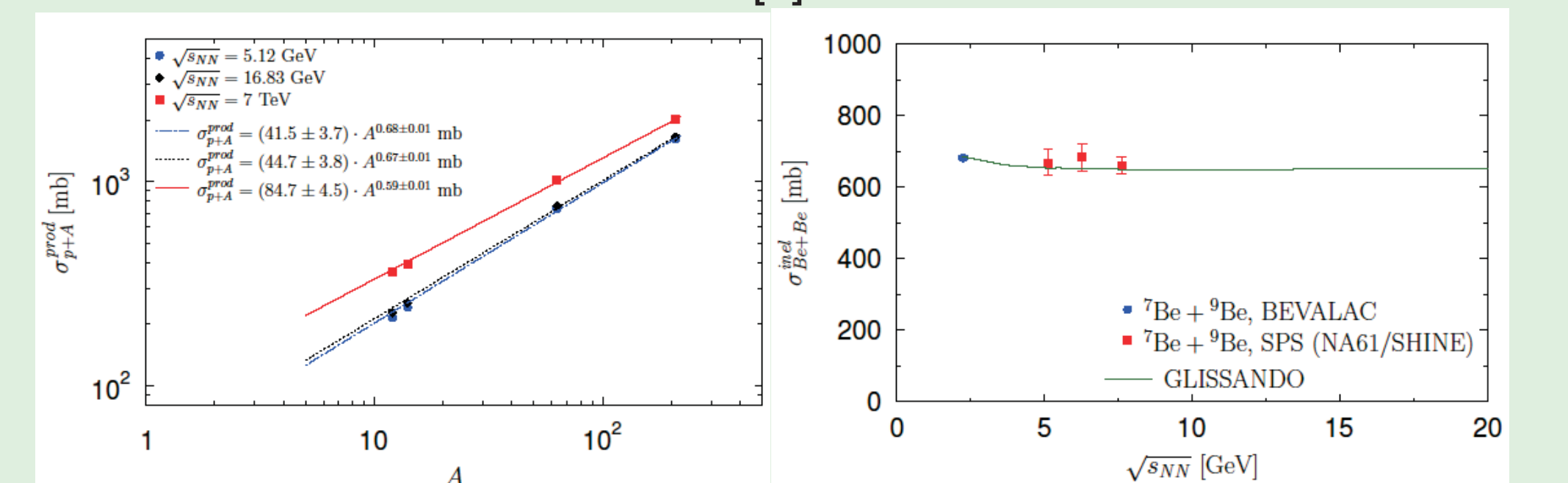


Fig.7 Left: Proton-nucleus production cross section $\sigma_{p+A}^{\text{prod}}$ as a function of target mass A . The results of GLISSANDO simulations for production reactions of protons with ^{12}C , ^{14}N , ^{63}Cu , ^{208}Pb ions at $\sqrt{s_{NN}} = 5.12, 16.83$ and 7000 GeV. **Right:** Inelastic cross section $\sigma_{\text{Be+Be}}^{\text{inel}}$ as a function of $\sqrt{s_{NN}}$. Results from BEVALAC (blue circles) [8] and SPS (NA61/SHINE) (red squares) [7] are compared with predictions of GLISSANDO.

References

- [1] W.Broniowski, M.Rybczyński, P.Bozek, Comput. Phys. Commun. 180, 69 (2009).
- [2] M.Rybczyński, G.Stefanek, W.Broniowski, P.Bozek, Comput. Phys. Commun., DOI:10.1016/j.cpc.2014.02.016.
- [3] <https://na61.web.cern.ch/na61/xc/index.html> and publications there
- [4] G.Antchev *et al.*, Europhys. Lett. 95, 41001 (2011).
G.Antchev *et al.*, Europhys. Lett. 101, 21002 (2013).
- [5] M.Rybczyński, W.Broniowski, and G.Stefanek, Phys. Rev. C 87, 044908 (2013).
- [6] M.Rybczyński, Acta Phys. Pol. B 45, 89 (2014).
- [7] I.Weimer, Bachelor Thesis, LMU Munich, 2013.
- [8] I.Tanihata *et al.*, Phys. Rev. Lett. 55, 2676 (1985).